

## Nanometric Resolution with Far-Field Optical Profilometry

S. Arhab,<sup>1</sup> G. Soriano,<sup>1</sup> Y. Ruan,<sup>1</sup> G. Maire,<sup>1</sup> A. Talneau,<sup>2</sup> D. Sentenac,<sup>3</sup> P. C. Chaumet,<sup>1</sup>  
K. Belkebir,<sup>1</sup> and H. Giovannini<sup>1</sup>

<sup>1</sup>*Aix-Marseille Université, CNRS, Centrale Marseille, Institut Fresnel, UMR 7249, 13013 Marseille, France*

<sup>2</sup>*Laboratoire de Photonique et de Nanostructures, CNRS, 91460 Marcoussis, France*

<sup>3</sup>*European Gravitational Observatory, 56021 Cascina (PI), Italy*

(Received 10 April 2013; published 2 August 2013)

We show experimentally that a resolution far beyond that of conventional far-field optical profilometers can be reached with optical diffraction tomography. This result is obtained in the presence of multiple scattering when using an adapted inverse scattering algorithm for profile reconstruction. This new profilometry technique, whose resolution can be compared to that of atomic microscopes, also gives access to the permittivity of the surface.

DOI: [10.1103/PhysRevLett.111.053902](https://doi.org/10.1103/PhysRevLett.111.053902)

PACS numbers: 42.30.Wb, 41.20.-q, 42.25.Fx

Determining the topography of surfaces at the nanoscale is a crucial issue in different domains ranging across optics, mechanics, nanotechnology, and surface science. Depending on the required resolution and on the conditions of observation, different types of interaction between the probe and the sample can be used. A subnanometer resolution can be reached with scanning electron microscopes (SEMs). The main drawback in this case is that the sample must be placed in vacuum and, in certain cases, depositing a thin layer of metal on the surface is necessary. In near-field scanning optical microscopes, a tapered optical fiber placed in the vicinity of the surface couples out the evanescent components of the field that carry out information on the subwavelength details of the profile. However, the coupling between the local probe and the sample makes the topography difficult to retrieve from these data. In atomic force microscopes (AFMs) a tip having a radius of curvature of a few nanometers is in contact with the sample. This technique provides nanometric resolution; however, its implementation is restrictive to a laboratory environment. Optical profilometers based on far-field reflectance measurements [1–5] may circumvent the problems mentioned above. However, their lateral resolution is limited by diffraction. Moreover, accurate results can only be obtained if the scattering from the surface can be approximated by single reflections from horizontal tangent planes, which is relevant only when slopes of the profile are small.

In view of these considerations, developing a new non-contact optical profilometry technique having subwavelength resolution, capable of dealing with randomly rough profiles while giving also the value of the dielectric constant of the surface, appears to be of high interest for a wide range of applications. Recent progress in optical diffractive tomographic microscopy (ODTM) has shown that this quantitative metrology technique can be very powerful for imaging three-dimensional objects [6,7]. In ODTM, the modulus and the phase of the scattered far field are measured for various incidence angles. A numerical

inversion algorithm is then applied to determine the opto-geometrical parameters (shape, permittivity distribution within the sample) from the scattered far-field data. The scattering regime plays a key role in the performances in terms of resolution. In the single scattering regime, the resolution limit is given by the Rayleigh-Abbe criterion. It has been demonstrated that this limit can be strongly overcome when multiple scattering becomes predominant [8–10]. In this case numerical inversion algorithms based on a rigorous resolution of Maxwell's equations must be used. Recently preliminary numerical simulations have demonstrated [11,12] the potentialities of ODTM applied to profilometry.

In this Letter we develop a profilometry setup based on an ODTM configuration. We show that, in the presence of multiple scattering, resolutions far beyond those obtained with far-field optical profilometers are obtained. We show in particular that using a nonlinear inversion algorithm based on a rigorous theory of surface scattering is the key for obtaining resolutions beyond the Rayleigh-Abbe criterion. We compare reconstructed profiles to those measured with electronic and atomic force microscopes and we show that the permittivity of the surface can be determined with the same setup.

The setup is depicted in Fig. 1 [13]. The light emitted at 632.8 nm by a 10 mW HeNe laser is divided in two parts. The first part is sent to the sample, which is illuminated by parallel beams whose angles of incidence  $\theta_{\text{inc}}$  can be varied thanks to the rotation of the mirror. For each incidence angle  $\theta_{\text{inc}}$ , the reflected diffracted far-field  $E_d$  is collected for various observation angles  $\theta_d$  by the microscope objective (Zeiss Epiplan-Apochromat 50 $\times$  with numerical aperture NA = 0.95 in air). An image is obtained in the focal plane of  $L_3$ . The second beam is spatially filtered by a pinhole to generate an aberration-free collimated reference wave. The reference beam is superimposed, through the beam splitter BS<sub>3</sub>, to the image field coming from the sample. An off-axis digital hologram of the diffracted field

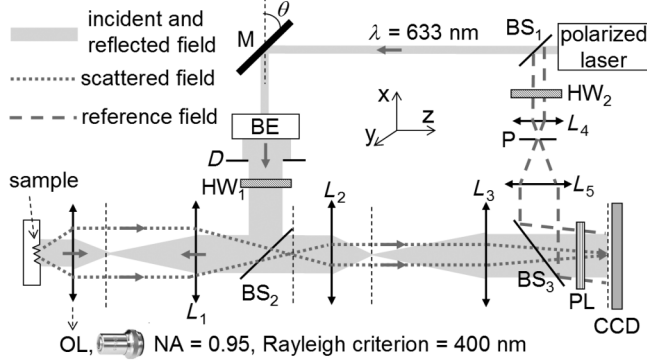


FIG. 1. Schematic of the full-polarized ODTM setup.  $M$  is the rotative mirror.  $BE$  is the beam expander.  $D$  is the diaphragm.  $P$  is the pinhole.  $BS$  is the beam splitter.  $OL$  is the objective lens.  $L_1$  is the tube lens.  $L_2$  and  $L_3$  are the relay lenses ( $f' = 3.5$  cm and 20 cm, respectively).  $HW_1$  and  $HW_2$  are the half-wave plates on the incident field and reference field, respectively, to measure in the TE or TM configuration. Polarizer  $PL$  can be rotated in order to perform ellipsometric measurements on the specular reflected beam.

is then recorded on a CCD camera (Kappa PS4-1020) placed in the focal plane of the lens  $L_3$ . The polarization of the incident beam and of the reference one can be adjusted thanks to the half-wave plates  $HW_1$  and  $HW_2$ . It is then possible to study the cases of the TE and TM polarizations. Polarizer  $PL$  can be rotated in order to perform ellipsometric measurements on the reflected specular beams. In this Letter we limit our study to samples invariant along the  $y$  axis. In this case the electromagnetic problem of scattering in TE and in TM polarization can be split in two scalar cases.

Once the measurements of the scattered fields  $E_d$  are carried out for various incidence angles, the surface profile is reconstructed using an inverse scattering algorithm. Under single scattering models such as the Kirchhoff-Fraunhofer (KF) or Born approximations, the surface profile is derived by applying inverse Fourier transformations of the measured scattered fields [14,15]. When multiple scattering is predominant, the inverse scattering problem is traditionally expressed as an optimization problem solved iteratively. The Newton-Kantorovitch (NK) iterative procedure is one of the techniques that solve the inverse scattering problem [16–18]. The basic idea underlying the NK method is to retrieve gradually the surface profile by minimizing a cost functional describing the discrepancy between the measurement and the field that would be obtained via the scattering forward rigorous model [16]. Assume that the scattered field  $E_d$  is linked to the surface, parametrized by the height  $h$ , through the scattering operator  $\mathbf{A}$

$$E_d^l = \mathbf{A}^l h, \quad (1)$$

where the superscript  $l = 1, \dots, L$  indexes the  $L$  incidence angles for which the scattered field is measured. At the  $i$ th

iteration step, the estimation of the surface profile is corrected from the previous one  $h_i = h_{i-1} + \delta h_i$  where the correction  $\delta h_i$  is the mean least square solution of

$$\delta E_d = \mathbf{D} \delta h_i. \quad (2)$$

The Fréchet derivative  $\mathbf{D}$  is determined by solving an adjoint forward scattering problem. Details of the derivation of  $\mathbf{D}$  for the perfectly conducting case are reported in Refs. [11,12,18]. In the present Letter, the derivation of  $\mathbf{D}$  is extended to the case of surfaces having a finite relative permittivity  $\epsilon$ . Hence, we have expressed the Fréchet derivative for a given contrast of permittivity  $\chi = \epsilon - 1$ . The residual error on the scattered field  $\delta E_d^{m,l}$ , for an incident angle  $\theta_i$  and a scattering angle  $\theta_m$ , writes as a contour integral over the profile  $\Gamma$ . For the TE polarization case, two total fields  $E_\Gamma^l$  and  $\tilde{E}_\Gamma^m$  on  $\Gamma$  are involved. The field  $E_\Gamma^l$  is the solution of the forward problem with the incidence angle  $\theta_i$ , while  $\tilde{E}_\Gamma^m$  is the solution of an adjoint scattering problem with angle  $-\theta_m$ . The variation of the scattered field with respect to the variation of the height  $h$  of the surface  $\Gamma$ , expressed symbolically in Eq. (2), takes the following explicit form

$$\delta E_d^{m,l} = k^2 \chi \int_\Gamma E_\Gamma^l \tilde{E}_\Gamma^m \delta h d\Gamma, \quad (3)$$

where  $k = 2\pi/\lambda$  is the wave number in vacuum. For the TM polarization case, both the normal and tangential derivatives of the two fields  $E_\Gamma$  and  $\tilde{E}_\Gamma$  on  $\Gamma$  are involved instead of the fields and

$$\delta E_d^{m,l} = \int_\Gamma \left( \chi \partial_n E_\Gamma^l \partial_n \tilde{E}_\Gamma^m + \frac{\chi}{1+\chi} \partial_t E_\Gamma^l \partial_t \tilde{E}_\Gamma^m \right) \delta h d\Gamma, \quad (4)$$

where  $\partial_n$  and  $\partial_t$  denote the normal and the tangential derivative of the relevant field, respectively. As described in Ref. [12], to improve the resolution, we first apply the NK algorithm to the TE-polarized data using as the initial guess a plane. The final result is used as the initial estimate for the inversion of the TM-polarized data.

Different normalization steps are done in order to calibrate the setup. Measurements are firstly made on the specular reflection of a reference flat surface of known permittivity. Here we have used a flat silicon sample (permittivity  $\epsilon = 15.1 + 0.15i$ ). The measurement of the intensity distribution on the camera for the different angles of incidence allows us to determine the incident intensity distribution on the sample. This information will be used to normalize the measured scattered amplitudes. Ellipsometric measurements performed at a known incidence angle by rotating polarizer  $PL$  [19] permit us to determine the unknown complex reflection and transmission coefficients of the optical components present between the source and the camera. Then the sample under investigation is placed in the setup. We assume that the amplitude of the field scattered from the sample in the specular direction is negligible compared to the amplitude

of the specular reflection. This assumption is valid when the size of the corrugated region is negligible compared to the size of the illuminated surface. It is therefore well adapted to the samples studied here that consist of grooves of small dimensions etched in an indium phosphate (InP) substrate. The permittivity of the InP surface is determined from the ellipsometric normalized measurements made on the specular beam. In order to compensate for possible phase fluctuations between the successive illuminations caused by random variations of the optical path, the measured phase of the scattered field for each illumination angle is shifted so that the phase in the specular direction is set to the argument of the Fresnel reflection coefficient of the flat surface.

A linear inversion under the Born approximation is first applied. In this case, the scattering sources (here the grooves) can be reconstructed from a simple inverse Fourier transform. Although not valid here, this approximation is useful to obtain a coarse reconstruction of the sample and defines an appropriate domain of investigation for the NK algorithm. The surface to be reconstructed can then be assumed flat outside of this domain. This approach also permits us to correct a residual defocus of the data set due to an imperfect adjustment of the camera in the image plane. This correction is required in order to set the phase origin in the NK algorithm.

In the calculations and in the experiments we have considered grooves etched on an InP surface. We have obtained experimentally a value of the permittivity  $\varepsilon = 13.6 + 1.5i$  which is close to the value that can be found for bulk InP at 632.8 nm. We used 22 incidences with angles  $\theta_{\text{inc}}$  varying between  $\pm \theta_{\text{inc}}^{\text{max}} = 55.6^\circ$  and 313 observation angles  $\theta_d$  varying between  $\theta_d^{\text{max}} = 58.4^\circ$ . This corresponds to a numerical aperture of illumination and collection  $\text{NA} \approx 0.85$ . The profiles of the samples have been measured with an electron microscope which will be considered as the reference measurement. Measurements have also been made with a scanning white light optical profilometer (ZYGO NewView 7300,  $\text{NA} = 0.85$ ) and with an AFM (Park Systems XE100, Nanoworld NCH tip). The samples considered in this Letter are composed of sets of grooves chemically etched on an InP surface with a HCl/H<sub>3</sub>PO<sub>4</sub> mixture (1:3) in the [011] direction. The slopes of the grooves are oriented at  $45^\circ$  with respect to the  $z$  axis.

The first sample is made of two trapezoidal grooves of width  $3 \mu\text{m}$  and  $2 \mu\text{m}$  at the bottom, of height 130 nm, and separated by  $2 \mu\text{m}$ . Figure 2 shows the results of the reconstructions obtained with the KF approximation (dot dashed line) and with the NK method (dashed line). As expected, for this sample the KF approximation gives satisfactory results. Indeed, for these lateral dimensions and for this aspect factor, scattering can be approximated by reflections on horizontal planes. This is confirmed by the accuracy of the reconstruction obtained with the Zygo

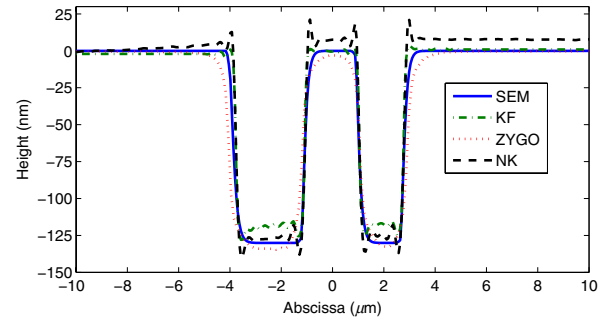


FIG. 2 (color online). The solid line shows the profile given by the SEM. The reconstructed profile given by the KF algorithm (dot dashed line), the Zygo profilometer (dotted line), and NK algorithm (dashed line).

profilometer (dotted line). The reconstruction with the NK method is also very close to the reference profile. In order to test the performances of the ODTM profilometer, we have considered a sample with three triangular grooves of width 200 nm at the surface, with a depth of 80 nm, and separated by 200 nm. In Fig. 3 we show in color scale the reconstruction obtained with the Born approximation, which assumes single scattering. This approach can only reconstruct the scattering sources on the substrate, and not directly the profile of the sample. The transverse resolution is  $1.22\lambda/(4\text{NA}) = 227 \text{ nm}$  at  $\lambda = 632.8 \text{ nm}$ . This method can locate the grooves but is unable to retrieve the profile of the surface.

From the results of Fig. 4(a) one can see that, as expected, the KF approximation cannot be applied in this case. Indeed, the optogeometrical parameters (slopes at  $45^\circ$ , dimensions much smaller than the diffraction limit) of the sample lead to multiple scattering effects that are not described accurately by approximated theories of diffraction. The Zygo profilometer also fails in retrieving the shape of the object. Indeed, the orientations of the slopes at  $45^\circ$  with respect to the optical axis strongly modify the optical path of the reflected part of the field. In addition the dimensions of the grooves are far below the resolution limit given by the numerical aperture of the system. Thus,

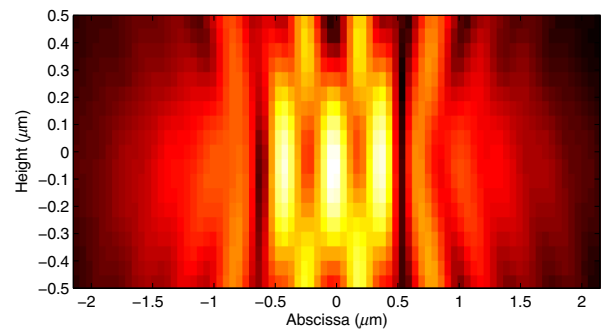


FIG. 3 (color online). Fourier transform of the scattered data measured in TM polarization. The profile under study is given in Fig. 4(a) (solid line). The color scale is in arbitrary units.

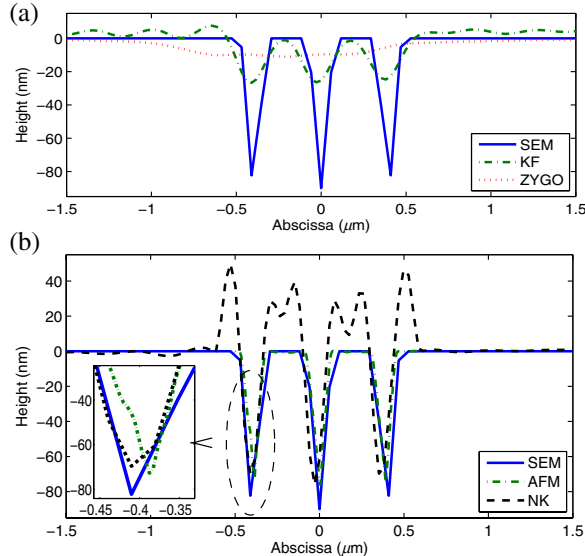


FIG. 4 (color online). The reference profile given by the SEM is plotted in (a) and (b) as a solid line. (a) Reconstruction given by KF method (dot dashed line) and Zygo profilometer (dotted line). (b) Reconstruction given by NK algorithm (dashed line) and AFM (dot dashed line).

scattering cannot be described by reflections on horizontal planes. When the ODTM measurements are processed with the NK method [see the dashed line in Fig. 4(b)] the profile is retrieved with a very good accuracy that can be compared to that of AFM measurements [see the dot dashed line in Fig. 4(b)], in particular at the bottom of the grooves. The resolution obtained in this case is far better than the Rayleigh criterion. However at the top of the surface, on each side of the grooves, residual bumps appear in the reconstructed profile. In order to understand the origin of these bumps we have made numerical simulations with different numerical apertures of illumination and collection. Figure 5 shows that the higher the numerical aperture is, the better is the accuracy.

The origin of the super resolution obtained in TM polarization with the ODTM profilometer has been discussed in previous papers [11,12]. The long-range

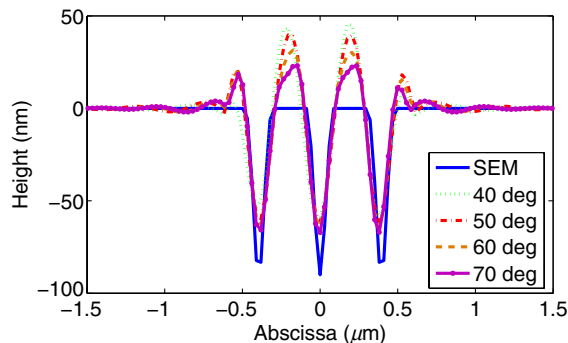


FIG. 5 (color online). Reconstructions given by NK algorithm for different maximum angles of illumination and collection.

interactions produced by multiple scattering within the metallic surface lead to a strong coupling between the spatial frequencies of the field. The propagating components of the field carry information on the high spatial frequencies. This information, which is taken into account by the model of diffraction in the NK method of reconstruction, permits us to retrieve the subwavelength details of the object. Moreover the NK method is compatible with the use of *a priori* information. For instance, to enhance the quality of the reconstruction, one may use prior information stating that the height  $h$  is negative in order to avoid the bumps reported in Fig. 5. The same kind of *a priori* knowledge has been successfully used in ODTM [20].

In conclusion, ODTM coupled to a NK reconstruction algorithm can provide a resolution that is out of reach of all optical profilometers working in far field. This technique gives also the value of the surface permittivity. We believe that the results presented in this Letter pave the way to the development of a new optical profilometry technique.

This work has been financed by the ANR SURMITO. The authors acknowledge A. Ronda of IM2NP for the AFM measurements. The ZYGO profilometer handled by C. Hecquet was acquired within the framework of the Espace Photonique facility and funded by the French Department of Industry, the Région PACA, and the European Community. The authors thank the unknown reviewers for their constructive suggestions that have improved the quality of the Letter.

- 
- [1] C. J. Brakenhoff, P. Blom, and P. Barends, *J. Microsc.* **117**, 219 (1979).
  - [2] D. Huang, E. A. Swanson, C. P. Lin, J. S. Shuman, W. G. Stinson, W. Chang, M. R. Hee, T. Flotte, K. Gregory, C. A. Puliafito, and J. G. Fujimoto, *Science* **254**, 1178 (1991).
  - [3] T. Wilson and C. J. R. Sheppard, *Theory and Practice of Scanning Optical Microscopy* (Academic, New York, 1984).
  - [4] G. Q. Xiao, T. R. Corle, and G. S. Kino, *Appl. Phys. Lett.* **53**, 716 (1988).
  - [5] H. J. Tiziani and H. M. Uhde, *Appl. Opt.* **33**, 1838 (1994).
  - [6] O. Haeberlé, K. Belkebir, H. Giovannini, and A. Sentenac, *J. Mod. Opt.* **57**, 686 (2010).
  - [7] W. Choi, C. Fang-Yen, K. Badizadegan, S. Oh, N. Lue, R. R. Dasari, and M. S. Feld, *Nat. Methods* **4**, 717 (2007).
  - [8] G. Maire, F. Drsek, J. Girard, H. Giovannini, A. Talneau, D. Konan, K. Belkebir, P. C. Chaumet, and A. Sentenac, *Phys. Rev. Lett.* **102**, 213905 (2009).
  - [9] F. Simonetti, *Phys. Rev. E* **73**, 036619 (2006).
  - [10] J. Girard, G. Maire, H. Giovannini, A. Talneau, K. Belkebir, P. C. Chaumet, and A. Sentenac, *Phys. Rev. A* **82**, 061801 (2010).
  - [11] S. Arhab, G. Soriano, K. Belkebir, A. Sentenac, and H. Giovannini, *J. Opt. Soc. Am. A* **28**, 576 (2011).

- [12] S. Arhab, H. Giovannini, K. Belkebir, and G. Soriano, *J. Opt. Soc. Am. A* **29**, 1508 (2012).
- [13] The experiment was automatized using the free software OpticsBenchUI (see <http://www.opticsbenchui.com/>).
- [14] N. Destouches, C. A. Guérin, M. Lequime, and H. Giovannini, *Opt. Commun.* **198**, 233 (2001).
- [15] E. Cuche, P. Marquet, and C. Depeursinge, *Appl. Opt.* **38**, 6994 (1999).
- [16] L. Tsang, J. A. Kong, K. H. Ding, and C. O. Ao, *Scattering of Electromagnetic Waves: Numerical Simulations*, Wiley Series in Remote Sensing (Wiley, New York, 2001).
- [17] O. M. Mendez, A. Roger, and D. Maystre, *Appl. Phys. B* **32**, 199 (1983).
- [18] A. Roger, *IEEE Trans. Antennas Propag.* **29**, 232 (1981).
- [19] R. M. A. Azzam, K. Bashara, *Ellipsometry and Polarized Light* (North-Holland, Amsterdam, 1977).
- [20] P. C. Chaumet, K. Belkebir, and A. Sentenac, *J. Appl. Phys.* **106**, 034901 (2009).